World Journal of Environmental Research
ISSN 2301-2641
Volume 15, Issue 1, (2025) 42-64

www.wjer.eu

Experimental and CFD analysis of diesel engine emissions and combustion characteristics with premixed gasoline fuel

Marsyeh Hoseionpur[a], Ferdowsi University of Mashhad, Mashhad, Iran.
Mohammad G. Rasul[b1], Central Queensland University, Queensland 4702, Australia. m.rasul@cqu.edu.au
Rahim Karami [c], Central Queensland University, Queensland 4702, Australia.
I. Jahirul [d], Central Queensland University, Queensland 4702, Australia.
Nur Hassan [e], Central Queensland University, Cairns, Queensland 4780, Australia.

Suggested Citation:
Hoseionpur, M., Rasul M. G., Karami R., Jahirul I., & Hassan N. (2025). Experimental and CFD analysis of diesel engine emissions and combustion characteristics with premixed gasoline fuel. *World Journal of Environmental Research, 15*(1), 42-64. https://doi.org/10.18844/wjer.v15i1.9728

Received from June 16, 2024; revised from February 22, 2025; accepted from April 23, 2025.
Selection and peer review under the responsibility of Prof. Dr. Haluk Soran, Near East University, Cyprus.

Abstract

This study investigates the effects of gasoline-premixed fuel on emissions and combustion characteristics in a compression ignition engine. A multi-cylinder, four-stroke diesel engine was analyzed using both experimental and computational methods. Emission and combustion parameters were measured at varying loading conditions for two gasoline–diesel blends and compared with pure diesel at a constant engine speed. Numerical simulations were conducted using the AVL Fire-CHEMKIN coupler for emission and combustion modeling, while CHEMKIN was used for chemical reaction modelling. Simulated results were validated against experimental data, showing minor deviations in mean effective pressure and emissions. The in-cylinder pressure data exhibited strong agreement with experimental results. The gasoline–diesel blends demonstrated longer ignition delays compared to pure diesel, influencing combustion characteristics. Additionally, the mole fraction of unburned hydrocarbons increased with gasoline blending. These findings provide insights into alternative fuel applications for compression ignition engines, contributing to advancements in fuel efficiency and emission reduction strategies.

Keywords: Computational fluid dynamics ; diesel engine emissions; diesel engine performance; premixed gasoline fuel

* ADDRESS FOR CORRESPONDENCE: Mohammad G. Rasul, School of Engineering and Technology, Central Queensland University, Queensland 4702, Australia. *E-mail address*: m.rasul@cqu.edu.au / Tel.: +61 402431669

1. INTRODUCTION

Given the current state of energy consumption and pollution, a key concern for internal combustion engines is the exhaust emission and fuel efficiency (Jin et al., 2022). As a result, researchers have concentrated their efforts on these two crucial aspects. Nowadays, the heavy-duty transportation sector and global industries heavily rely on diesel engines. In diesel engines, fuel is directly injected into the cylinder close to the top dead Centre of the piston, parts of the cylinder have a rich fuel mixture while other parts have a lean mixture, leading to the formation of soot and nitrogen oxides, respectively. To simultaneously reduce these pollutants in diesel engines, researchers and manufacturers have consistently explored the use of alternative fuels such as light fuels (alcohol and gasoline), methane, biogas, and biodiesel (Wen et al., 2022). Various methods like blending, fumigation, dual fuel, and direct use can facilitate the application of alternative fuels in diesel engines (Palash et al., 2013; Martins and Brito, 2020).

Different dual fuel operation approaches can be applied to diesel and light fuels. Fumigation and mixing are the most often utilized techniques. Alcohol fuels are combined with diesel fuel in the blending procedure prior to being injected into the cylinder (Navanth & Sharma 2025). Additional chemicals are needed to stabilize the miscibility of combining alcohol with diesel fuel. As a result, the quantity of alcohol that can be used for blending operations is restricted (Ghadikolaei 2016). According to Martos et al., (2023), alcohol fumigation is the simple process of injecting, carburetting, or spraying alcohol fuel into the intake air upstream of the manifold. The benefit of this introduction technique is that it allows for the distribution of the entire fuel supply premixed with the intake air, hence increasing air usage. It allows a large percentage of alcohol fuels to be used in engine operation because no additives are needed to stabilize the miscibility of alcohol and diesel fuel. The engine is only slightly modified by adding a lowpressure fuel injector, separate fuel tank, lines, and controls. Consequently, the engine's efficiency in fumigation mode will improve. These factors have led to the widespread application of alcohol fumigation, particularly ethanol fumigation, in DI diesel engines. Only a few investigations on gasoline fumigation in DI diesel engines have been found in the relevant literature, despite the abundance of studies on alcohol fumigation (El-Sheekh et al., 2023; Sahu et al., 2022).

It is widely recognized that gasoline is not considered an alternative fuel, as it is primarily used in spark-ignition engines. Nevertheless, when used as an additive to diesel fuel through various techniques, gasoline has shown favorable results in terms of engine performance and exhaust emissions (Sahin et al., 2012; Kumaravel et al., 2024). Given the limitations of using gasoline in compression ignition engines, recent research has focused on partially replacing diesel fuel with gasoline, either through fumigation or premixed injection into the air intake. These methods, which involve either modifying the fuel composition or making minor engine adjustments, can be easily implemented in existing diesel engines. Recently, numerous experimental and some theoretical studies (Sahin & Durgun 2007a; Durghan et al., 2009; Hoseinpour et al., 2018; Imran et al., 2013) have investigated the fumigation of light fuels such as gasoline, ethanol, and methanol in compression ignition engines. Studies conducted by Park et al., (2014, 2016); Sahin & Durgun (2007a, 2007b, 2013); and Sahin et al., (2008, 2012) have investigated the impact of diverse premixed injection source ratios of bioethanol and gasoline on the exhaust emission and combustion characteristics of diesel engines, across a range of operating conditions. Without offering an ideal state, most researchers have examined for NOx, UHC, CO, soot, braking thermal efficiency, specific fuel consumption, and exhaust gas temperature. However, there are a few computational fluid dynamics (CFD) studies or numerical analyses

available on light fuel fumigation in diesel engines, despite the necessity of using advanced engineering tools to investigate and evaluate these proposed technologies.

The key to optimizing the internal combustion engine is based on a correct understanding of the combustion process. It should be noted that the processes inside the engine cylinder (especially the combustion cycle) are so complex that a series of empirical relationships and reasonable assumptions are needed for their complete modeling (Tay et al., 2017). Multidimensional combustion modeling methods, which are often called computational fluid dynamics (CFD) models, can provide detailed information about the spatial distribution of gas velocity, pressure, temperature, and other properties inside the combustion chamber during the combustion process. In these models, a set of conservation equations of mass, momentum, energy, and chemical species are solved numerically as basic partial differential equations corresponding to appropriate initial and boundary conditions. Using computational fluid dynamics models, engine performance and production pollutants emissions can be well simulated (Tian & Abraham 2014).

In a CFD model, when paired with detailed chemical kinetics and accurately defined initial and boundary conditions, and it consistently uses the results of both detailed chemical kinetics and fluid models, the developed model becomes the most precise model for simulating diesel engines with alternative fuels to biodiesel (Jiaqiang et al., 2016), homogeneous charge compression ignition (HCCI) engines (Yousefi & Birouk 2016), reactivity-controlled compression ignition (RCCI) engines (Li et al., 2016; Salahi et al., 2017), dual fuel diesel engines (Yousefi & Birouk 2017), and partially premixed compression ignition engines (Esfahanian et al., 2017). These models have consistently drawn the attention of internal combustion engine researchers. In these models, temperature and concentration distributions within the cylinder are modeled alongside mass and energy transfer due to fluid movement (especially turbulence), with the effects of cylinder geometry considered. One of the pioneering software in this area is AVL FIRE, which has gained popularity among researchers due to its graphical interface. Therefore, studies utilizing the AVL-CHEMKIN coupling have demonstrated that a suitable mechanism can significantly enhance the accuracy of pollutant prediction, making its use highly recommended over traditional CFD alone. However, a review of existing research indicates that theoretical studies on the fumigation of light fuels, especially gasoline, in diesel engines are limited (Sahin et al., 2007b; Durghan et al., 2009). These studies typically use quasi-dimensional models and focus only on combustion and performance characteristics, without considering pollutant trends.

1.1. Purpose of study

Therefore, in alignment with the aim of this research to develop an accurate model for dual-fuel diesel engine combustion in fumigation mode and predict its associated pollutants and combustion parameters, this study investigates the proposed solution using numerical methods, specifically integrating CFD with chemical kinetics. Initially, the emission and combustion behaviors were experimentally tested and subsequently compared with simulated results obtained using the AVL-CHEMKIN coupler. A range of benefits can be assessed through the CFD model for the turbulent combustion of gasoline fumigation in an internal combustion engine, providing manufacturers and policymakers with valuable performance references for their engines.

2. MATERIAL AND METHOD

2.1. Experimental setup and procedure

This study used a four-cylinder, 4-stroke diesel engine. Table 1 specification of test engine. The schematic diagram of the experimental setup is shown in Figure 1. The engine's air intake manifold included four fuel injectors and a gasoline fuel rail incorporated into it. To produce a low gasoline/air mixture, gasoline was fed into the intake manifold at a pressure of 0.3 MPa. Fuel for the injectors was supplied by a fuel pump that was controlled by an electronic control unit. Engine speed and torque could be adjusted thanks to the hydraulic dynamometer that was attached to the engine. An electronic balance was used to measure fuel usage with a precision of 0.01 g. An AVL Ditest1000 online exhaust gas analyzer was used to track various gaseous emissions, such as smoke opacity, NO, CO, CO_2, and UHC. A PT100 thermocouple sensor was used to detect the temperature of the exhaust gas.

Table 1

Engine details

Engine brand	Motorsazan-Iran G4.248
Engine type	Naturally aspired, water-cooled
Operating principle	Four stroke, direct injection
Number of cylinders	Inline four cylinders
Fuel injection pump	Mechanically controlled in rotary type
Rated power, Kw	56 kW at 2000rpm
Rated torque, Nm	290 Nm at 1300 rpm
Bore × Stroke	101 × 127 mm
Compression ratio	16:1
Injection timing	336
Intake valve opening	713
Intake valve closing	213
Exhaust valve opening	485
Exhaust valve closing	5

Figure 1

Diagram schematic for the engine experiment setup

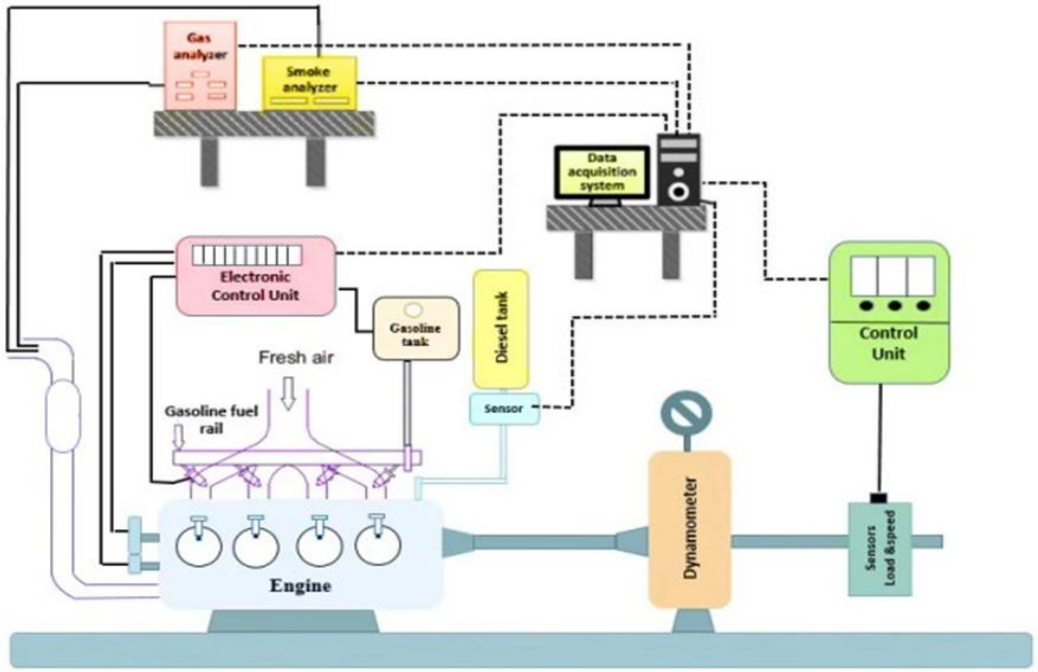

Figure 1 includes the following parts:

1	engine	9	intake manifold
2	dynamometers	10	diesel injectors
3	dynamometer sensors	11	engine speed and camshaft sensor
4	control unit	12	exhaust port
5	gas analysers	13	gasoline tank
6	smoke analyser	14	diesel tank
7	electronic control unit	15	diesel flow meter
8	fuel common rail	6	data acquisition system

In every operational mode, the engine was operated for several minutes until the exhaust gas temperature, lubricating oil temperature, and cooling water temperature stabilized. After reaching these steady-state conditions, data were collected. Gaseous emissions were measured continuously for 2 minutes, average values reported. Each test was repeated thrice, with results showing consistency within a 95% confidence level. The details of the measurement accuracy and apparatus are listed in Table 2.

Table 2

A list of measuring precision

Measurement Load	unit	Measurement range	Accuracy±
	Nm	350	0.1
Speed	rpm	0-7000	1
Fuel flow measurement	gr	0-6000	0.01

Air flow Measurement	m/s	0-20	0.03
Temperature	°C	0-1200	1
Crank angle encoder	rpm	0-5000 rpm	1
Time	s	-	-
NO emission	ppm	0-5000	1
HC emission	ppm	0-30000	1
CO emission	%	0-15	0.01
CO2 emission	%	0-20	0.01
Smoke	m-1	0-10	0.01

The engine was operated under steady-state conditions at different brake mean effective pressures (BMEPs), corresponding to approximately 25%, 50%, and 75% of full load at 1300 rpm, which is the speed at which maximum torque is achieved. Diesel fuel served as the baseline fuel, while gasoline was introduced as a fumigation fuel in two different mass flow rates (0.35 kg/h and 0.7 kg/h) at each testing point. The experiments were conducted under the engine operated solely on diesel fuel ("Diesel") and the engine operated on diesel fuel as the primary fuel, with gasoline used as a fumigation fuel ("D+FG").

At each engine speed, the rate of gasoline flow was consistent across both cases. Thus, three types of fuel were tested under each operational condition, identified in figures and tables as "Diesel," "D+FG1," and "D+FG2." Detailed operational parameters for each mode and the mass consumption rates of the main fuel (diesel) and gasoline are documented in Table 3.

Table 3

Details of test cases examined

Test condition	**Operation mode**	**Gasoline mass flow rate kg/ h**	**Main fuel mass flow rate kg/ h**	**Air/fuel Ratio** -
n=1300 rpm	Diesel	0	2.41 1.91	61.89 58.64
Load=25%	D+FG1	0.35	1.84	60.19
bmep=2.1 bar	D+FG2	0.70		
n=1300 rpm	Diesel	0	4.03	39.51
Load=50%	D+PG1	0.35	3.56	37.15
bmep=4.2 bar	D+PG2	0.70	3.28	37.05
n=1300 rpm	Diesel	0	5.86 5.15	24.28 23.68
Load=75%	D+PG1	0.35	5.00	24.08
bmep=6.2 bar	D+PG2	0.70		

2.2. Numerical simulation

To simulate the engine's in-cylinder flow field, combustion process, and emission production, this work integrates a chemical kinetics solver (CHEMKIN) with AVL Fire, a full 3-D computational fluid dynamics (CFD) software. The solver used in this study employed averaged conservation equations for mass, momentum, enthalpy, and species concentrations. Turbulence effects are accounted for using a compressible version of the standard k–ε turbulence model. To simulate wall heat transfer in diesel engines, appropriate models are employed. Specifically, the standard wall function model is utilized, which accommodates variations in gas density and incorporates the turbulent Prandtl number within boundary layers (Beale and Reitz, 1999). This approach allows for the consideration of the complex engine wall heat exchange processes during simulations.

In compression ignition (CI) engines, ignition and combustion processes are primarily governed by chemical kinetics phenomena. Therefore, accurate modeling of chemical kinetics mechanisms is crucial for achieving precise simulations. Detailed chemical kinetic mechanisms from external sources can be integrated into CFD codes to comprehensively cover features of combustion and processes involved in the creation of emissions in engines. To establish a connection between the CFD solver and the chemistry solver, AVL-FIRE software provides initial species concentrations, pressure, and temperature for each computational cell to the CHEMKIN solver. The chemistry solver solves systems of chemistry-related equations to determine species formation rates and the corresponding heat release for all computational cells, while the CFD code solves the averaged transport equations.

In other words, the CFD solver finds the temperature, pressure, and species concentrations in each cell by solving transport equations at each computational time step. The CHEMKIN solver receives this data after which it is coupled internally with the CFD solver in the software framework. This integrated approach ensures that both fluid dynamics and chemical kinetics aspects are effectively modeled and synchronized throughout the simulation process. Figure 2 illustrates how fuel chemistry influences the initial conditions of each time step within the software, utilizing a singleregion zero-dimensional model for each computational cell. The software integrates chemical equations and reaction coefficients from a text file, encompassing stoichiometric reactions and kinetic coefficients.

In the present work, the mechanism developed by Raw and Ritz in 2008 is selected to symbolize the chemical reactions connected to combustion (Ra and Reitz, 2008). With 45 species and 142 chemical reactions, it is an optimized reduced detailed chemical reaction mechanism that provides comparatively faster CPU times for computing workloads when compared to other mechanisms with similar capabilities. Normal heptane chemical species C7H16 has been used as a substitute for diesel fuel and isooctane species C8H18 has been used for gasoline fuel. To perform the modeling, in the initial conditions, it is assumed that a mixture of air and gasoline (three types of isooctane, oxygen and nitrogen) is distributed in the entire combustion chamber with certain ratios. Then, at the start of SOI injection, the second diesel fuel is injected into the combustion chamber. In this study, the simulation adopts the perfect gas assumption to estimate the thermodynamic properties of the gas mixture. This assumption simplifies the calculation of gas behavior by assuming ideal gas behavior, which is adequate for capturing the overall thermodynamic behavior in the context of the simulations conducted.

Figure 2

The process of solving the combination of multi-dimensional CFD model with fuel chemical kinetics

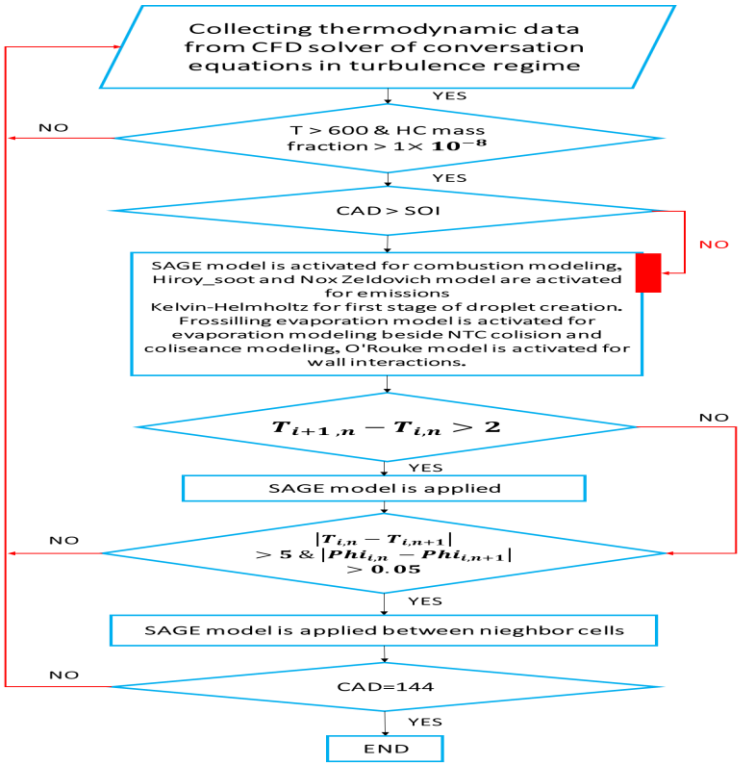

Source: Hoseinpour et al., (2024).

2.3. In-cylinder geometry configurations

Utilizing the engine specifications and geometric maps of the piston, a numerical mesh was constructed for simulation within the ESE Diesel environment of the software. Figure 3 displays a depiction of the generated mesh at two positions: top dead center and bottom dead center. To optimize grid calculations and account for the symmetrical geometry of the engine combustion chamber, grid refinement was focused on a 90-degree section. This approach was sufficient for accurate simulations in this study. The generated numerical mesh consisted of 11,382 cells at top dead center and 54,453 cells at bottom dead center of the engine. To investigate the combustion process, simulations were conducted on a closed engine cycle, spanning from intake valve closure (IVC) to exhaust valve opening (EVO). This comprehensive approach allows for detailed analysis of combustion dynamics and performance characteristics within the simulated engine environment. In this study, the closing time of the intake valves provided the initial conditions for the numerical solution. This data included initial temperature, initial pressure, and the composition percentages of oxygen (O2), nitrogen (N2), and octane (C8H18) as part of an air and premixed gasoline mixture, derived from laboratory measurements.

Figure 3

Computational meshes for the investigated geometry at TDC and BDC

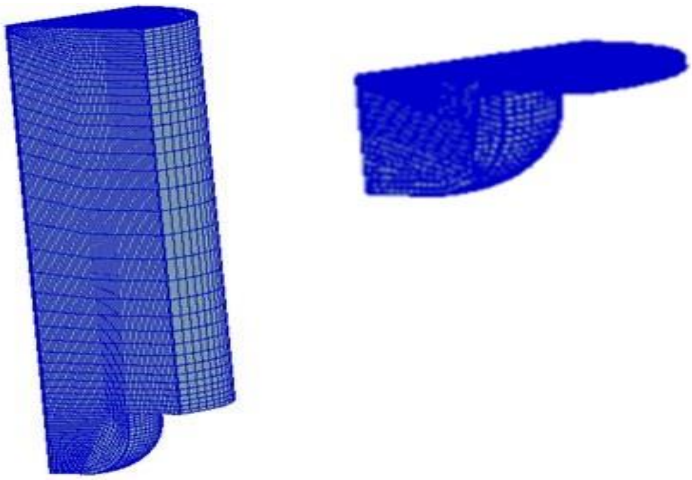

Establishing accurate boundary conditions for the generated geometry is crucial. Based on experimental cooling water temperatures, the cylinder wall was assigned a temperature of 470 Kelvin, while the piston and cylinder head surfaces were set at 570 Kelvin. Figure 4 illustrates the specific areas on the numerical grid where these boundary conditions were applied. This approach ensures that the simulation reflects real-world conditions as closely as possible, enhancing the reliability and accuracy of the computational model used in the study. The Specification of boundary conditions are explained in Table 4.

Figure 4

Specification of boundary conditions in numerical network

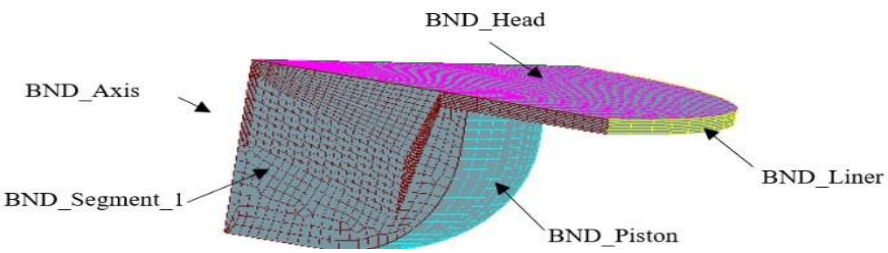

Table 4

Specification of boundary conditions in numerical network

Name	Name in Figure2	Color	Type	Boundary condition
Piston surface	BND_Piston	Light blue	wall	Moving mesh
wall	BND_Liner	yellow	wall	Constant speed
Symmetry axis	BND_Axis	red	Symmetry	
Symmetry section	BND_Segment_1	brown	Inlet/outlet	periodic
Head cylinder	BND_Head	pink	wall	Constant speed

The grid independence analysis, conducted based on the criterion of maximum pressure inside the cylinder at 25% maximum load and 1300 rpm, revealed that results obtained with 11,382 grids exhibited a

negligible difference (less than 1%) compared to those obtained with 17,325 grids. Therefore, for practical purposes and considering computational efficiency, the number of grids was chosen as 11,382. This number was deemed sufficient to achieve accurate simulation results within an acceptable calculation time frame.

3. RESULTS

3.1. Model validation

A few findings from the experimental setup are used to validate numerical results via in-cylinder pressure and exhaust emission. The engine was operated with diesel as the primary fuel and gasoline as the fumigated fuel that was injected in the intake manifold. At engine IVC, the temperature and in-cylinder pressure was measured and found to be, respectively, 355 K and 1.2 bar. To examine the presented model, the model was validated with the experimental values of the pressure inside the cylinder. The in-cylinder pressure graphs obtained from the experiment and simulation in three states with different loads are compared with each other. In all three modes, the engine works in pure diesel conditions and the selected loads are 25%, 50%, and 75% of the maximum load at 1300 rpm respectively. Figure 5 shows a comparison of the measured and computed in-cylinder pressure curves. The experimentally measured and numerically calculated data are found to agree well, and the model's computational prediction of the engine's maximum pressure value and the start of combustion time is found to be within an acceptable range of the experimental test data. For a more complete comparison, the measured and predicted values of the mean effective pressure as well as their percentage differences for all three modes of pure diesel fuel are presented in Table 5. This table shows that the maximum difference between the experimental and numerical average effective pressures is less than 8%. The following section presents a comparison of the measured and projected emission levels. It can be observed that the model accurately depicts the trend in emissions of NO, CO, CO_2, and UHC.

Table 5

Percentage difference of mean effective pressure values in simulation and laboratory mode

	Numerical result			Experimental result			Percent error		
Load (% of full load)	25%	50%	75%	25%	50%	75%	25%	50%	75%
mep	1.9	4.04	6.29	2.1	4.1	6.2	7.1	1.5	1.4

Figure 5

A comparison between computed and measured pressure a) 25% b)50% and c)75% of full loads

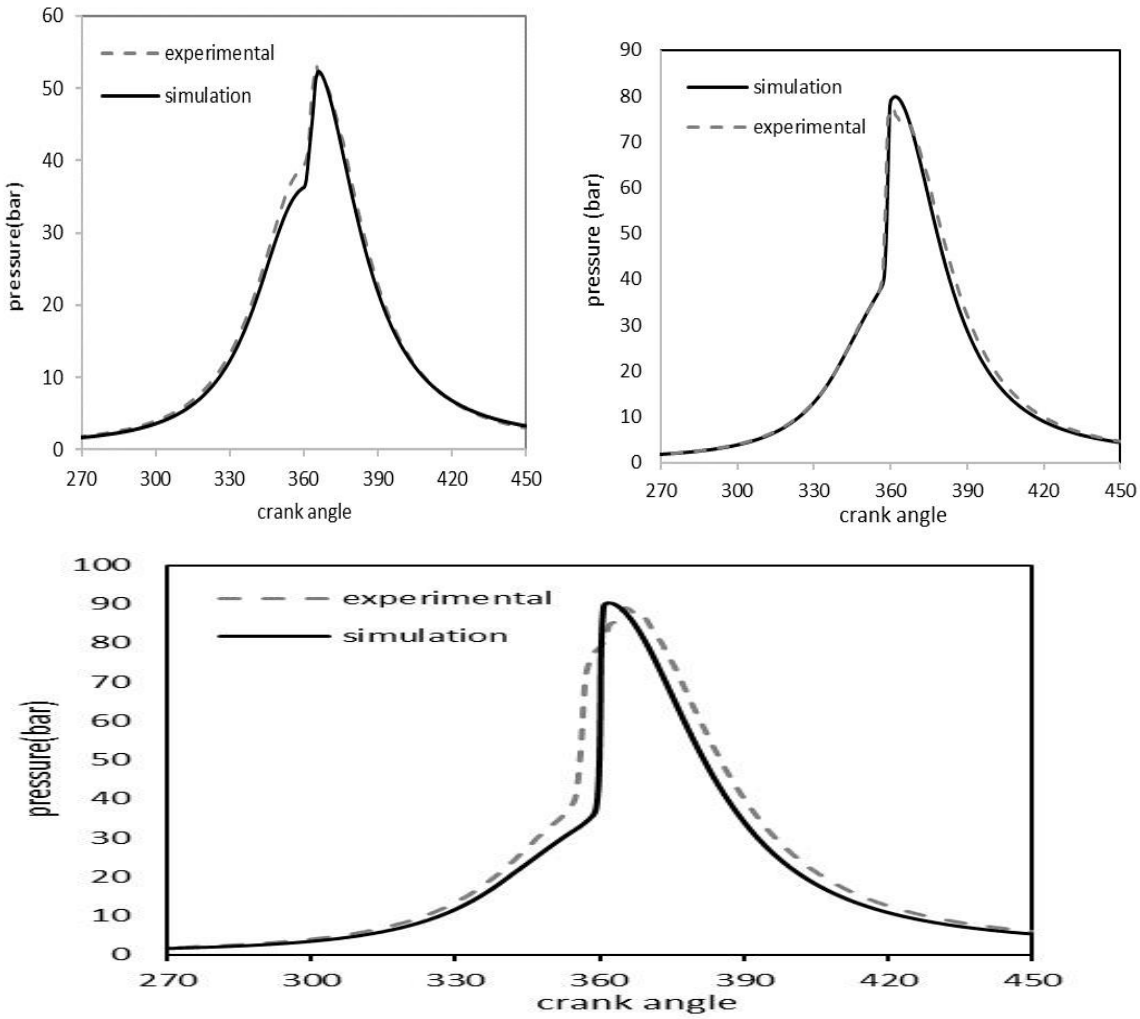

3.2. Simulation of combustion parameters

For a better understanding of the combustion process, the graphs of in-cylinder pressure heat release rate and average in-cylinder temperature in terms of crank angle for all three simulated modes are shown in Figures 6, 7, and 8. As can be seen in Figure 6, in all three simulated loads, the pressure curve of fumigation modes is close to pure diesel mode, but gasoline fumigation caused a delay in the start of combustion and a decrease in the maximum pressure inside the cylinder. For example, in the condition of 50% loading, the maximum pressure value in three modes D, D+FG1, and D+FG2 is 82.70, 78.6, and 76.3 bar, respectively, at the angles of 720.2, 720.7 and 723.2 degrees. The delay in the start of combustion is the result of the low cetane number of gasoline fuel and also the increase in volumetric efficiency.

Figure 6

In-cylinder pressure versus the crank angle a) 25% (b)50% and (c)75% of full loads

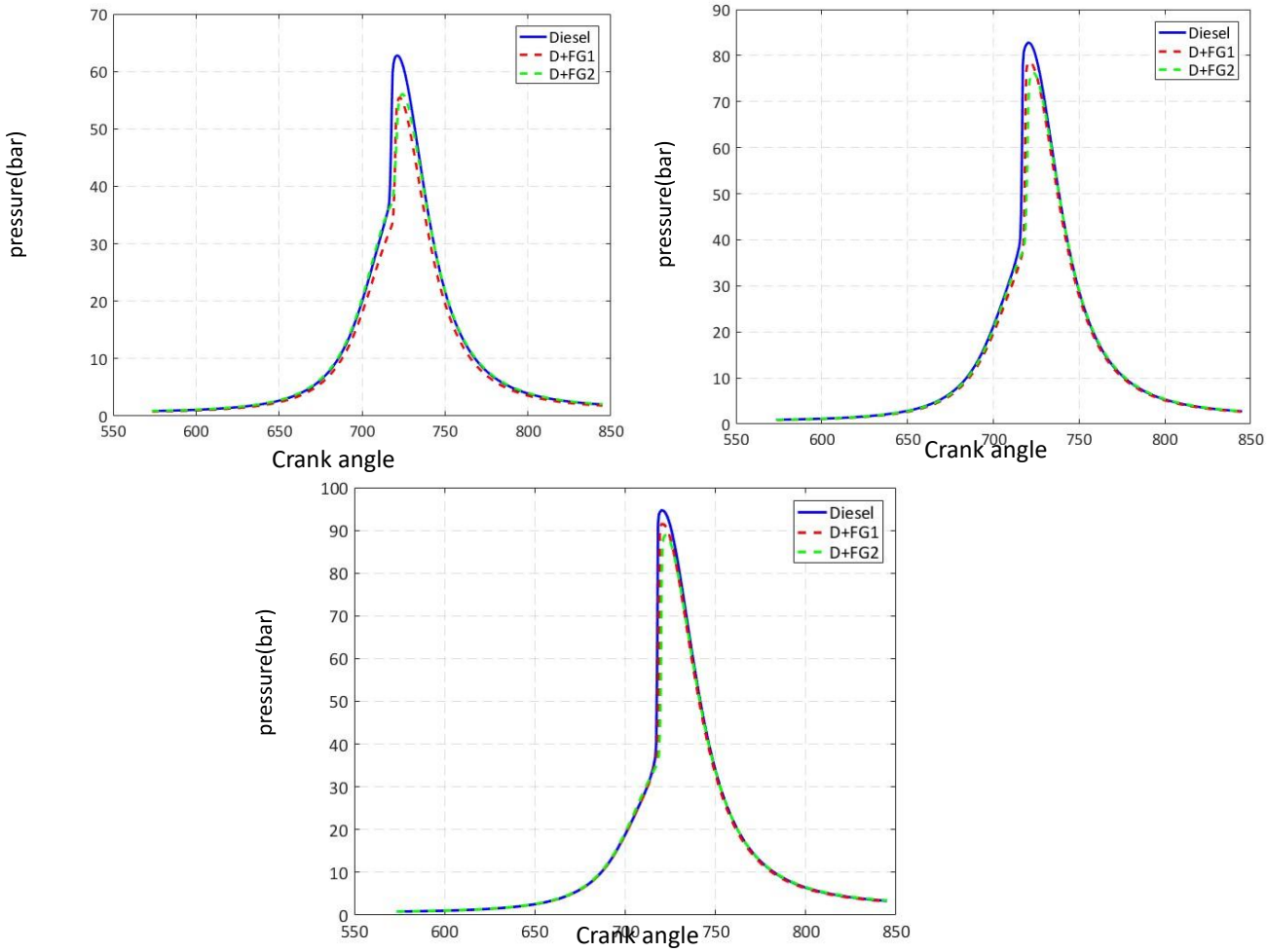

The comparison of the results in Figure 6 shows that at high loads, the reduction of the pressure inside the cylinder is less, which can be due to more complete combustion of the mixture of fuel and air inside the cylinder, and as a result, the combustion temperature is higher. Şahin et al., (2012) also showed that fumigation of gasoline at a speed of 2000 rpm under 50% load conditions will reduce the maximum pressure inside the cylinder.

Figure 7

The heat release rate versus the crank angle a) 25% b)50% and c)75% of full loads

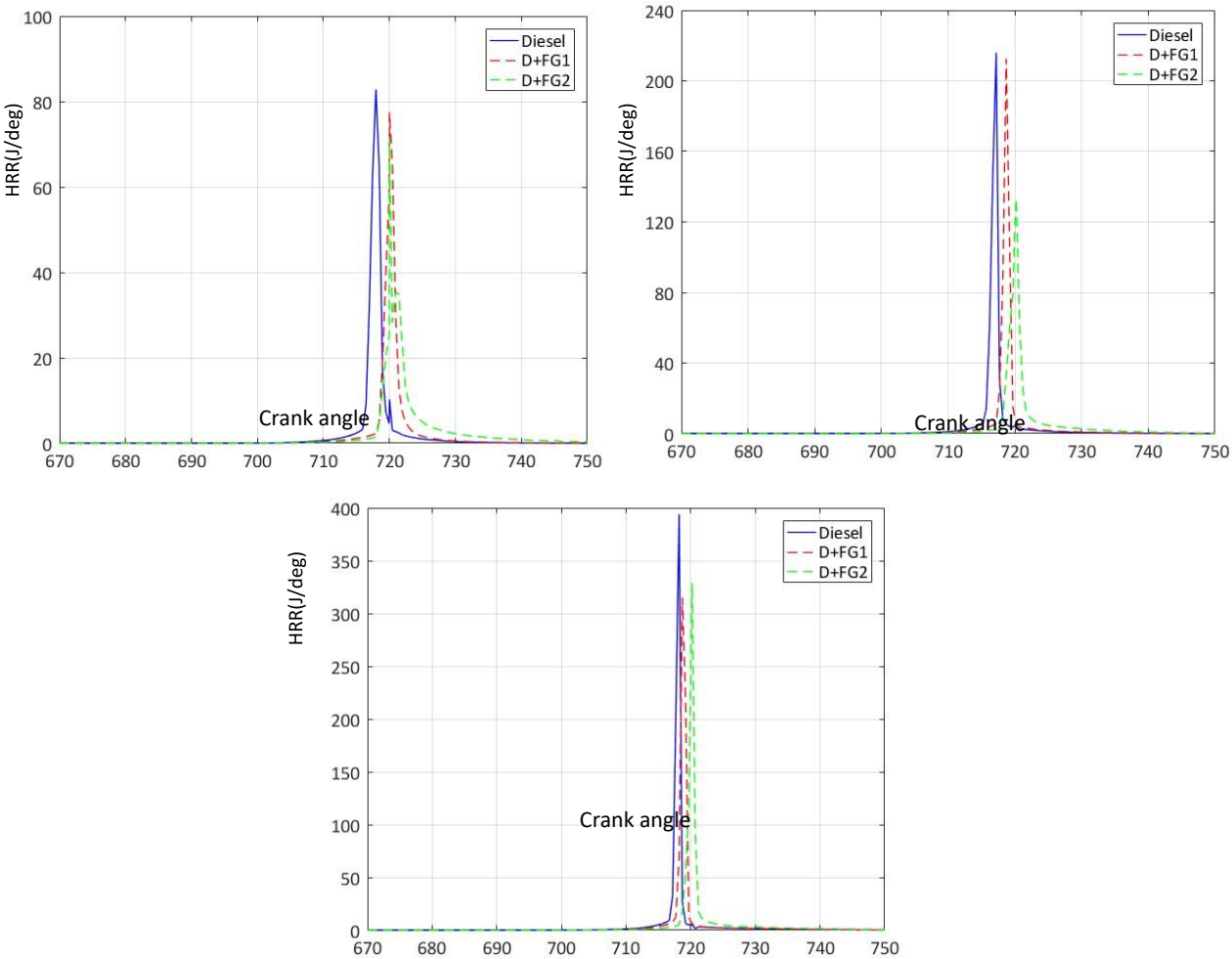

Regarding the changes in the heat release rate, Figure 7 shows that gasoline fumigation causes a delay in the ignition and a decrease in the heat release rate, which can be due to decrease in the cetane number of the final mixture inside the cylinder. In other words, as can be seen, the addition of gasoline reduces the reactivity and causes the heat release to start later, and the combustion time is slightly longer. In general, for all three loading conditions, fumigation modes have the widest heat release rate curve with the lowest maximum value. Reduction of the maximum heat release rate in ethanol fumigation mode, as well as dual fuel engine with gasoline and biodiesel fuel and bioethanol and biodiesel by other researchers have been reported in experimental studies (Sahin & Durgun 2013; Park et al., 2014; Ramachander et al., 2022). The effect of this issue can be seen in Figure 6 as the pressure curve rises late with the increase in the amount of added gasoline (due to the small percentage of fumigated fuel, the changes are minor). The changes in the

temperature inside the cylinder in Figure 8 also show that gasoline fumigation can cause the temperature to decrease during combustion. So, in the simulated conditions, this decrease was more noticeable at low loads. The experimental results also showed that the reduction of the percentage of nitrogen oxides was more at low loads. This decrease in temperature can also be due to the increase in the specific heat capacity of the mixture in the fumigation mode and as a result, the decrease in the heat release rate. Temperature reduction for ethanol and n-butanol in the fumigation and dual-fuel mode has also been reported in experimental studies (sahin et al., 2015).

Figure 8

The in-cylinder temperature versus the crank angle a) 25% b)50% and c)75% of full loads

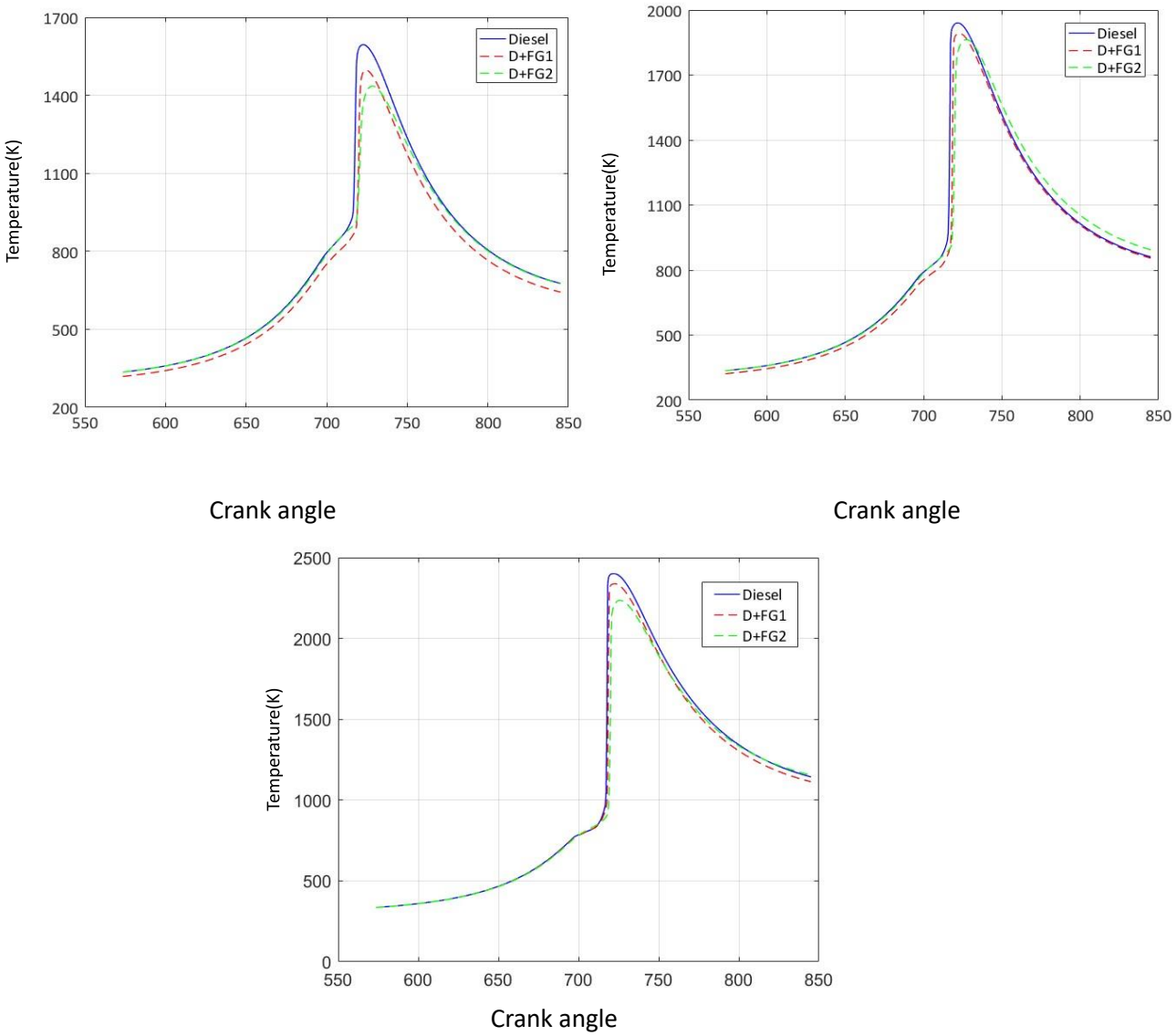

3.3. Exhaust emission parameters

The variation of unburned hydrocarbons, nitrogen oxide, and carbon monoxide in the present study is reported in Figure 9, Figure 10, Figure 11, and Table 6. For this purpose, the mole fraction of each of the mentioned gas species is taken as the output at the end of the simulation (the opening time of the outlet valve) and the changes in the amount of each pollutant in terms of mole fraction and according to the crank angle are presented and the simulation results were compared with the laboratory results in table 6. The difference between the simulation and laboratory results can be explained by the fact that the fuel used in the simulation is isooctane, while the fuel used in the experiments is gasoline. On the other hand, not considering the pressure reference in the engine suction system, and leakage from cylinder and piston seams, the accuracy of measuring devices can cause differences between numerical and experimental results. In general, it can be said that the simulation results have relatively good accuracy. But it is necessary to mention that the nature of the formation of pollutants in the engine is so complex that one should not expect answers with high accuracy from any model. Some of the experimental result at 50% of full load is shown in figure 9, figure 10 and figure 11 with color point.

Table 6

Comparison of emission exhaust between experimental and numerical results

emission	load	Simulation			experimental			Error percentage		
		Diesel	D+FG1	D+FG2	Diesel	D+FG1	D+FG2	Diesel	D+FG1	D+FG2
CO	25%	1.07E-03	2.36E-03	3.50E-03	8.00E-04	2.50E-03	3.90E-03	33.75%	5.76%	10.38%
	50%	3.68E-04	6.20E-04	1.41E-03	2.90E-04	7.00E-04	1.30E-03	26.93%	11.47%	8.35%
	75%	3.80E-04	5.88E-04	9.46E-04	5.00E-04	7.00E-04	9.00E-04	24.00%	16.00%	5.09%
CO2	25%	3.42E-02	3.45E-02	3.28E-02	3.51E-02	3.44E-02	3.15E-02	2.68%	0.25%	4.17%
	50%	5.11E-02	5.38E-02	5.26E-02	5.68E-02	5.65E-02	5.52E-02	10.03%	4.75%	4.76%
	75%	8.26E-02	7.82E-02	7.92E-02	9.00E-02	8.50E-02	8.73E-02	8.20%	7.98%	9.24%
NO	25%	5.09E-04	3.60E-04	2.89E-04	5.29E-04	3.43E-04	2.60E-04	3.78%	5.06%	11.19%
	50%	1.28E-03	1.16E-03	1.01E-03	1.20E-03	1.09E-03	1.02E-03	6.67%	6.91%	1.17%
	75%	2.38E-03	2.04E-03	1.75E-03	2.17E-03	1.93E-03	1.84E-03	9.68%	5.70%	4.89%
	25%	2.77E-05	1.77E-04	2.02E-04	2.80E-05	1.34E-04	1.64E-04	1.07%	32.09%	23.17%

UHC	50%	1.46E-05	7.98E-05	1.07E-04	1.80E-05	6.10E-05	8.90E-05	18.89%	30.82%	20.22%
	75%	9.30E-06	2.60E-05	3.29E-05	2.30E-05	5.90E-05	7.20E-05	59.57%	55.93%	54.31%

To explain the production of CO pollutants in the engine, Figure 9 shows the changes in the mass ratio of the chemical species of CO inside the cylinder according to the crank angle in different loading conditions. In these figures, the basic diesel mode and the two gasoline fumigation modes are compared with each other. As it can be seen, after the beginning of the combustion reactions (near the top dead point), relatively large amounts of CO species are produced in the intermediate reactions, and after reaching a maximum amount, it decreases due to the combination with oxygen and the production of carbon dioxide. If a small amount of this remains in the cylinder at the end of the combustion process, it reaches a constant value when the output valve opens and finally exits the engine as a pollutant. The comparison of the two modes of gasoline fumigation with the basic mode in Figure 8 shows that the use of gasoline causes a significant increase in carbon monoxide in the exhaust gases, and the increase in the fumigation ratio increases the amount of this pollutant in the exhaust gases (comparison of the two modes D+FG1 and D+FG2).

Figure 9

Carbon monoxide versus the crank angle 50% of full load at 1300rpm

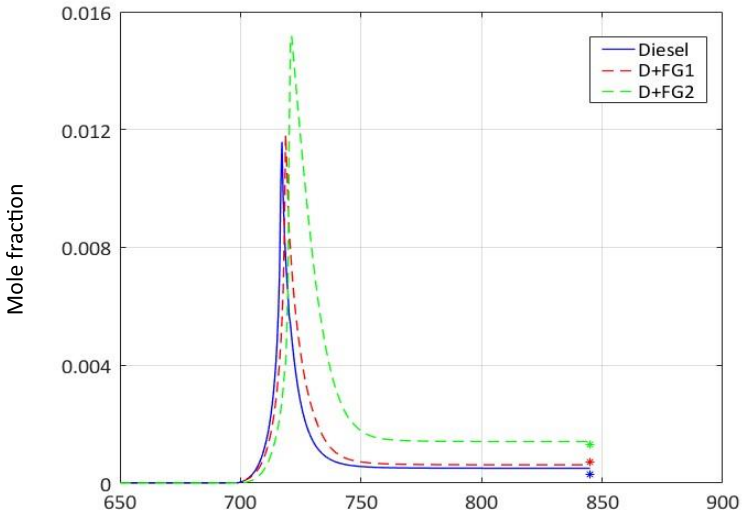

An increase in the amount of carbon monoxide in the exhaust gases can be a result of incomplete combustion due to a decrease in temperature for the combustion and a decrease in oxygen in the input mixture. The comparison of the results shows that the use of high amounts of gasoline fumigation can cause a delay in the combustion process and, as a result, further away from the complete state, so that the amount of carbon monoxide in the higher fumigation mode (D + FG2) will increase significantly compared to the pure

diesel mode. It should be noted, that the reported result in Figure 9 is obtained one for 50% and the trend of CO pollutant production for the other investigated modes at 25% and 75% of full load are like 50% of full load just with the difference that the amount of this increase in the fumigation mode is lower at high loads. This result can be obtained from the presented discussion that gasoline fumigation results in better conditions for the working mode of a very rich mixture of fuel and air, i.e., high engine loads. The reason for this is the higher combustion temperature in high load conditions.

Figure 10 shows the changes in the mass ratio of the NO chemical species inside the cylinder according to the crank angle at different loads. It can be seen, that the maximum value of NO occurs near the top rest point of the engine, where the temperature inside the cylinder is maximum. After that, due to chemical reactions and decomposition, its amount decreases until it remains almost constant until the end of the expansion course. In other words, when the combustion process starts and the temperature rises, nitrogen in the air reacts with oxygen and produces nitrogen oxide. Further, with the progress of the reactions, a small amount of NO production decreases and finally, the remaining amount is removed from the engine as a pollutant. A comparison of the results in Figure 10 shows that the use of gasoline fumigation causes a decrease in the temperature inside the cylinder for the combustion zone and a corresponding decrease in the production of nitrogen oxides. Also, in the case where the amount of fumigated gasoline is higher, lower amounts of nitrogen oxides are produced compared to lower amounts of vaporized gas. In such a way that the higher amount of fumigated gasoline (D+FG2) causes a lower amount of NO pollutant to be created at the end of the engine's working cycle, according to the pressure and heat release diagrams, it can be said that delayed ignition causes a decrease in the temperature in the engine and a decrease in the production rate of nitrogen oxides.

Figure 10

Nitrogen oxide versus the crank angle 50% of full load at 1300rpm *Crank angle*

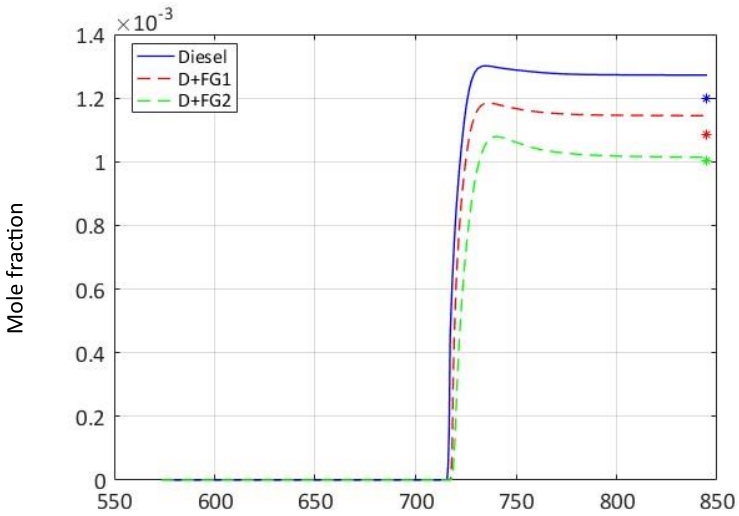

Changes in the mass ratio of CO_2 inside the cylinder according to the crank angle are shown in Figure 11. As can be seen, the maximum amount of carbon dioxide occurs near the top dead point due to higher temperature. In the combustion process, carbon monoxide is first formed in the reaction of hydrocarbons and air, and as the temperature inside the cylinder increases, carbon monoxide molecules will combine with this

gas and form carbon dioxide if there is enough oxygen. Therefore, because of these changes, as the top dead point is approached and the temperature inside the cylinder increases, the amount of this species increases, but after the combustion stage has passed and the temperature inside the cylinder decreases, the carbon monoxide molecules are no longer able to convert to carbon dioxide, and the amount of this species will remain constant.

Also, the comparison of the three different modes in Figure 11 also shows that the use of gasoline fumigation will reduce the amount of carbon dioxide produced, which can reduce the combustion temperature and movement towards incomplete combustion. By increasing the amount of fumigated gasoline, the reduction of carbon dioxide will also increase. Also, the comparison of the results in different loading modes shows that the changes in these loads are similar, with the difference that the percentage of changes in high loads will be lower, because of this the result is just shown in the 50% of full load. To calculate the concentration of unburned hydrocarbons, the concentration of all species including hydrogen and carbon (C_3H_7, C_2H_6) in the exhaust gases will be added together. The results of this section are presented in the form of mole fraction for three different states in each loading condition in Table 6. The obtained results show a significant increase of unburnt hydrocarbons in any loading conditions with gasoline fumigation. This increase agrees with the experimental results of this study and other studies.

Figure 11

Carbon dioxide versus the crank angle 50% of full load at 1300rpm

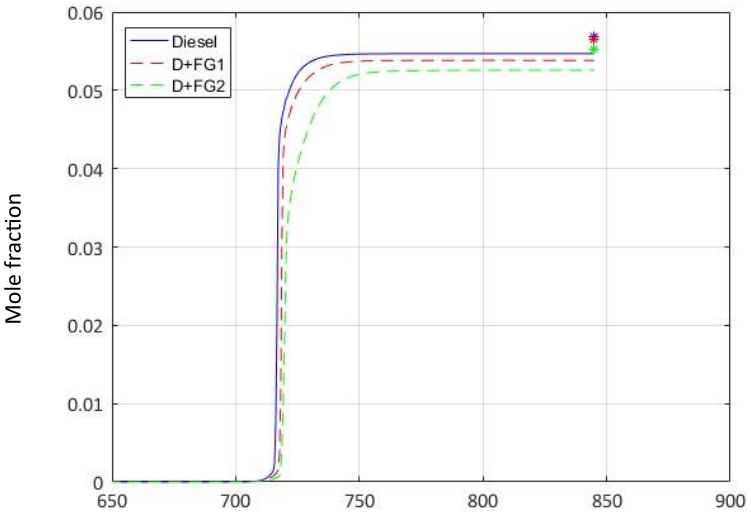

The simulated temperature distribution at 390° CA in the engine combustion chamber's central vertical part is depicted in Figure12a. The results are for D+FG2 at 25% of full load meaning the higher amount of gasoline fumigation in lower loads. The figure shows how the combustion process begins in the combustion chamber's core and moves throughout the chamber. Additionally, as seen in this Figure, the piston head's maximum temperature was 2551° C (Karami al., 2023). The NO mass fraction emissions at 390 °CA are depicted in the photographs in Figure12b. The region where the most NO is produced, in the middle of the combustion chamber at the top of the piston, is an intriguing feature of these pictures. The rationale is that

Figure12a shows that this is the location with the maximum temperature, and as the temperature rises, so does the amount of NO created, leading to the highest amount of NO being produced there. Determining the location and timing of the NO emissions' production can be aided by these pictures (Karami et al., 2021).

Figure 12

The progress of NO emissions' production

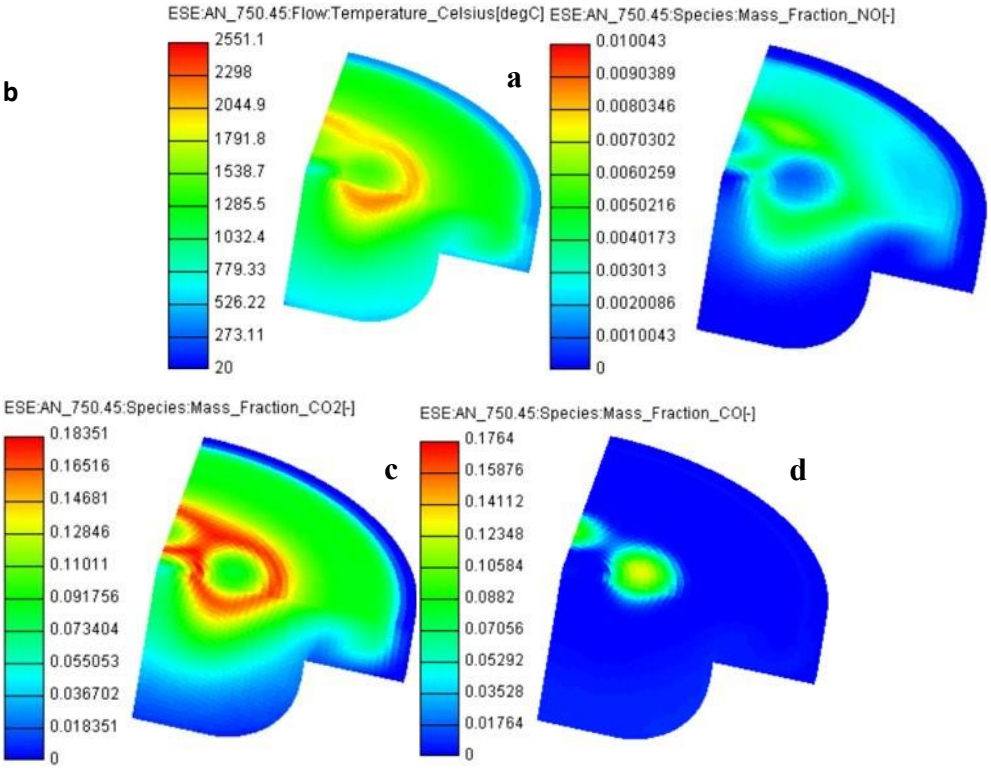

Note: (a) in-cylinder temperature (b) NO (c), CO (d) CO_2 at 30° ATDC at 1300 rpm and 25% Load.

4. DISCUSSION

The CO_2 emissions as mass fractions at 390 °CA are depicted in Figure12c. The formation of carbon dioxide and the spread of its density within the combustion chamber are depicted in this image. The fact that the combustion chamber's middle is where CO_2 production occurs is an intriguing observation. The site of CO_2 generation can be consistently ascertained by comparing this image with Figure 12a and understanding the temperature pattern within the combustion chamber. The reaction between CO and oxygen is facilitated by

raising the temperature. More CO_2 is created as a result. Put another way, more complete combustion results from a higher gas temperature. Moreover, the production of carbon dioxide increases with engine speed (Karami et al., 2022).

Figure 12d shows the photos of CO emissions as mass fractions at 390 CA. The location pattern of CO generation differs from that of CO_2 as seen in Figure12c. According to numerous studies, the interaction of CO with oxygen in the presence of heat is what produces CO_2 in the engine. Thus, it follows that there is an inverse relationship between the CO_2 and CO concentrations in the combustion chamber. The site of CO_2 generation in the combustion chamber is around the piston's boundaries, while CO is formed in the piston's core and at its top. The reason is that water is continuously circulated around the top of the chamber wall as part of a cooling system. As was already indicated, heat plays a significant role in the conversion of CO to CO2 because it slows down the oxidation of CO to CO_2 by reducing kinetic energy and resulting in fewer collisions between CO and O_2 gas molecules (Karami et al., 2020).

5. CONCLUSION

The combustion of a four-cylinder diesel engine equipped with a premixed fuel injection system was experimentally measured and simulated with AVL-CHEMKIN coupler and CFD. The results showed that the use of CFD coupling with chemical kinetics can be used as a suitable model to predict emission and combustion characteristics in the case of gasoline fumigation in a diesel engine. The maximum pressure in pure diesel mode was predicted with a maximum error of 2.6%, while this was less than 10% for CO, NOx, and CO_2 at higher load.

Generally, under the conditions of gasoline fumigation this model had a relatively good quantitative and qualitative agreement with the experimental results. In all three simulated loads, the pressure change curve of the vaporization modes is close to the pure diesel mode, and gasoline vaporization causes a slight delay in the start of combustion and a decrease in the maximum pressure inside the cylinder. Also, spraying gasoline causes ignition delay and decreases the rate of heat release and temperature during combustion.

Conflict of interest: No potential conflict of interest was reported by the authors.

Ethical Approval: The study adheres to the ethical guidelines for conducting research.

Funding: This research did not receive any specific grant from funding agencies in the public, commercial, or not-for-profit sectors.

REFERENCES

Beale, J. C., & Reitz, R. D. (1999). Modeling spray atomization with the Kelvin-Helmholtz/Rayleigh-Taylor hybrid model. *Atomization and sprays*, *9*(6). https://www.dl.begellhouse.com/journals/6a7c7e10642258cc,2b018a87685a3d87,76af95984924bb68.html

Durgun, O. R. H. A. N., & Şahin, Z. E. H. R. (2009). Theoretical investigation of heat balance in direct injection (DI) diesel engines for neat diesel fuel and gasoline fumigation. *Energy Conversion and Management*, *50*(1), 43-51. https://www.sciencedirect.com/science/article/pii/S0196890408003312

Hoseionpur, M., Rasul M. G., Karami R., Jahirul I., & Hassan N. (2025). Experimental and CFD analysis of diesel engine emissions and combustion characteristics with premixed gasoline fuel. *World Journal of Environmental Research, 15*(1), 42-64. https://doi.org/10.18844/wjer.v15i1.9728

El-Sheekh, M. M., El-Nagar, A. A., ElKelawy, M., & Bastawissi, H. A. E. (2023). Solubility and stability enhancement of ethanol in diesel fuel by using tri-n-butyl phosphate as a new surfactant for CI engine. *Scientific Reports*, *13*(1), 17954. https://www.nature.com/articles/s41598-023-45252-7

Esfahanian, V., Salahi, M. M., Gharehghani, A., & Mirsalim, M. (2017). Extending the lean operating range of a premixed charged compression ignition natural gas engine using a pre-chamber. *Energy*, *119*, 1181-1194. https://www.sciencedirect.com/science/article/pii/S0360544216317005

Ghadikolaei, M. A. (2016). Effect of alcohol blend and fumigation on regulated and unregulated emissions of IC engines—A review. *Renewable and Sustainable Energy Reviews*, *57*, 1440-1495. https://www.sciencedirect.com/science/article/pii/S1364032115015117

Hoseinpour, M., Karami, R., Salahi, M. M., Andwari, A. M., Gharehghani, A., & Garcia, A. (2024). *Influence of Intake Charge Temperature and EGR Rate on the Combustion and Emission Characteristics of Ammonia/Diesel Dual-Fuel Engine* (No. 2024-37-0025). SAE Technical Paper. https://www.sae.org/publications/technical-papers/content/2024-37-0025/

Hoseinpour, M., Sadrnia, H., Ghobadian, B., & Tabasizadeh, M. (2018). Effects of gasoline fumigation on exhaust emission and performance characteristics of a diesel engine with mechanically-controlled fuel injection pump. *Environmental Progress & Sustainable Energy*, *37*(5), 1845-1852. https://aiche.onlinelibrary.wiley.com/doi/abs/10.1002/ep.12852

Imran, A., Varman, M., Masjuki, H. H., & Kalam, M. A. (2013). Review on alcohol fumigation on diesel engine: a viable alternative dual fuel technology for satisfactory engine performance and reduction of environment concerning emission. *Renewable and Sustainable Energy Reviews*, *26*, 739-751. https://www.sciencedirect.com/science/article/pii/S1364032113003730

Jiaqiang, E., Liu, T., Yang, W. M., Li, J., Gong, J., & Deng, Y. (2016). Effects of fatty acid methyl esters proportion on combustion and emission characteristics of a biodiesel fueled diesel engine. *Energy Conversion and Management*, *117*, 410-419. https://www.sciencedirect.com/science/article/pii/S0196890416301522

Jin, C., Ampah, J. D., Afrane, S., Yin, Z., Liu, X., Sun, T., ... & Liu, H. (2022). Low-carbon alcohol fuels for decarbonizing the road transportation industry: a bibliometric analysis 2000–2021. *Environmental Science and Pollution Research*, *29*(4), 5577-5604. https://link.springer.com/article/10.1007/s11356-021-15539-1

Karami, R., Hoseinpour, M., Rasul, M. G., Hassan, N. M. S., & Khan, M. M. K. (2022). Exergy, energy, and emissions analyses of binary and ternary blends of seed waste biodiesel of tomato, papaya, and apricot in a diesel engine. *Energy Conversion and Management: X*, *16*, 100288. https://www.sciencedirect.com/science/article/pii/S2590174522001118

Karami, R., Rasul, M. G., & Khan, M. M. (2020). CFD simulation and a pragmatic analysis of performance and emissions of tomato seed biodiesel blends in a 4-cylinder diesel engine. *Energies*, *13*(14), 3688. https://www.mdpi.com/1996-1073/13/14/3688

Karami, R., Rasul, M. G., & Khan, M. M. K. (2023). An empirical and computational fluid dynamics analysis of combustion performance of a diesel engine fueled with tomato seed oil biodiesel. *Journal of Energy Resources Technology*, *145*(4), 041302. https://asmedigitalcollection.asme.org/energyresources/article-abstract/145/4/041302/1145941

Karami, R., Rasul, M. G., Khan, M. M. K., Salahi, M. M., & Anwar, M. (2021). Experimental and computational analysis of combustion characteristics of a diesel engine fueled with diesel-tomato seed oil biodiesel blends. *Fuel*, *285*, 119243. https://www.sciencedirect.com/science/article/pii/S0016236120322390

Hoseionpur, M., Rasul M. G., Karami R., Jahirul I., & Hassan N. (2025). Experimental and CFD analysis of diesel engine emissions and combustion characteristics with premixed gasoline fuel. *World Journal of Environmental Research, 15*(1), 42-64. https://doi.org/10.18844/wjer.v15i1.9728

Kumaravel, S., Saravanan, C. G., Vikneswaran, M., Raman, V., Sasikala, J., Js, F. J., ... & Allasi, H. L. (2024). Exploration of flame characteristics of gasoline engine fuelled by gasoline-pentanol blends using combustion endoscopy. *Scientific Reports*, *14*(1), 31692. https://www.nature.com/articles/s41598-024-81221-4

Li, J., Yang, W. M., & Zhou, D. Z. (2016). Modeling study on the effect of piston bowl geometries in a gasoline/biodiesel fueled RCCI engine at high speed. *Energy Conversion and Management*, *112*, 359-368. https://www.sciencedirect.com/science/article/pii/S0196890416000583

Martins, J., & Brito, F. P. (2020). Alternative fuels for internal combustion engines. *Energies*, *13*(16), 4086. https://www.mdpi.com/1996-1073/13/16/4086

Martos, F. J., Doustdar, O., Zeraati-Rezaei, S., Herreros, J. M., & Tsolakis, A. (2023). Impact of alcohol–diesel fuel blends on soot primary particle size in a compression ignition engine. *Fuel*, *333*, 126346. https://www.sciencedirect.com/science/article/pii/S0016236122031702

Navanth, A., & Sharma, T. K. (2025). High-fidelity simulation of emission characteristics in dual-fuel HCCI engines with premixed n-dodecane and ethanol as secondary fuel. *Journal of Thermal Analysis and Calorimetry*, 1-16. https://link.springer.com/article/10.1007/s10973-025-14030-0

Palash, S. M., Masjuki, H. H., Kalam, M. A., Masum, B. M., Sanjid, A., & Abedin, M. J. (2013). State of the art of NOx mitigation technologies and their effect on the performance and emission characteristics of biodiesel-fueled Compression Ignition engines. *Energy conversion and management*, *76*, 400-420. https://www.sciencedirect.com/science/article/pii/S0196890413004305

Park, S. H., & Lee, C. S. (2016). Effect of Bioethanol on Combustion and Exhaust Emissions in a Diesel–Bioethanol Dual-Fuel Combustion Engine. *Journal of Energy Engineering*, *142*(2), E4015009. https://ascelibrary.org/doi/abs/10.1061/(ASCE)EY.1943-7897.0000313

Park, S. H., Yoon, S. H., & Lee, C. S. (2014). Bioethanol and gasoline premixing effect on combustion and emission characteristics in biodiesel dual-fuel combustion engine. *Applied energy*, *135*, 286-298. https://www.sciencedirect.com/science/article/pii/S0306261914008678

Ra, Y., & Reitz, R. D. (2008). A reduced chemical kinetic model for IC engine combustion simulations with primary reference fuels. *Combustion and Flame*, *155*(4), 713-738. https://www.sciencedirect.com/science/article/pii/S0010218008001351

Ramachander, J., Gugulothu, S. K., & Sastry, G. R. K. (2022). Performance and emission reduction characteristics of metal based Sio2 nanoparticle additives blended with ternary fuel (Diesel-MME-Pentanol) on CRDI diesel engine. *Silicon*, *14*(5), 2249-2263. https://link.springer.com/article/10.1007/s12633-021-01024-4

Şahin, Z. E. H. R. A., Durgun, O. R. H. A. N., & Bayram, C. O. Ş. K. U. N. (2012). Experimental investigation of gasoline fumigation in a turbocharged IDI diesel engine. *Fuel*, *95*, 113-121. https://www.sciencedirect.com/science/article/pii/S0016236111006028

Şahin, Z. E. H. R. A., Durgun, O. R. H. A. N., & Bayram, C. O. Ş. K. U. N. (2008). Experimental investigation of gasoline fumigation in a single cylinder direct injection (DI) diesel engine. *Energy*, *33*(8), 1298-1310. https://www.sciencedirect.com/science/article/pii/S0360544208000649

Şahin, Z., & Durgun, O. (2013). Improving of diesel combustion-pollution-fuel economy and performance by gasoline fumigation. *Energy conversion and management*, *76*, 620-633. https://www.sciencedirect.com/science/article/pii/S0196890413004391

Hoseionpur, M., Rasul M. G., Karami R., Jahirul I., & Hassan N. (2025). Experimental and CFD analysis of diesel engine emissions and combustion characteristics with premixed gasoline fuel. *World Journal of Environmental Research, 15*(1), 42-64. https://doi.org/10.18844/wjer.v15i1.9728

Şahin, Z., & Durgun, O. R. H. A. N. (2007a). High speed direct injection (DI) light-fuel (gasoline) fumigated vehicle diesel engine. *Fuel*, *86*(3), 388-399. https://www.sciencedirect.com/science/article/pii/S0016236106002833

Şahin, Z., & Durgun, O. R. H. A. N. (2007b). Theoretical investigation of effects of light fuel fumigation on diesel engine performance and emissions. *Energy Conversion and Management*, *48*(7), 1952-1964. https://www.sciencedirect.com/science/article/pii/S0196890407000507

Şahin, Z., Durgun, O., & Aksu, O. N. (2015). Experimental investigation of n-butanol/diesel fuel blends and n-butanol fumigation–evaluation of engine performance, exhaust emissions, heat release and flammability analysis. *Energy conversion and management*, *103*, 778-789. https://www.sciencedirect.com/science/article/pii/S0196890415006512

Sahu, T. K., Shukla, P. C., Belgiorno, G., & Maurya, R. K. (2022). Alcohols as alternative fuels in compression ignition engines for sustainable transportation: A review. *Energy Sources, Part A: Recovery, Utilization, and Environmental Effects*, *44*(4), 8736-8759. https://www.tandfonline.com/doi/abs/10.1080/15567036.2022.2124326

Salahi, M. M., Esfahanian, V., Gharehghani, A., & Mirsalim, M. (2017). Investigating the reactivity controlled compression ignition (RCCI) combustion strategy in a natural gas/diesel fueled engine with a pre-chamber. *Energy Conversion and Management*, *132*, 40-53. https://www.sciencedirect.com/science/article/pii/S0196890416310147

Tay, K. L., Yang, W., Li, J., Zhou, D., Yu, W., Zhao, F., ... & Mohan, B. (2017). Numerical investigation on the combustion and emissions of a kerosene-diesel fueled compression ignition engine assisted by ammonia fumigation. *Applied Energy*, *204*, 1476-1488. https://www.sciencedirect.com/science/article/pii/S0306261917303409

Tian, Z. F., & Abraham, J. (2014). Application of computational fluid dynamics (CFD) in teaching internal combustion engines. *International Journal of Mechanical Engineering Education*, *42*(1), 73-83. https://journals.sagepub.com/doi/abs/10.7227/IJMEE.42.1.7

Wen, M., Yin, Z., Zheng, Z., Liu, H., Zhang, C., Cui, Y., ... & Yao, M. (2022). Effects of different gasoline additives on fuel consumption and emissions in a vehicle equipped with the GDI engine. *Frontiers in Mechanical Engineering*, *8*, 924505. https://www.frontiersin.org/articles/10.3389/fmech.2022.924505/full

Yousefi, A., & Birouk, M. (2016). Fuel suitability for homogeneous charge compression ignition combustion. *Energy Conversion and Management*, *119*, 304-315. https://www.sciencedirect.com/science/article/pii/S0196890416303077

Yousefi, A., & Birouk, M. (2017). Investigation of natural gas energy fraction and injection timing on the performance and emissions of a dual-fuel engine with pre-combustion chamber under low engine load. *Applied Energy*, *189*, 492-505. https://www.sciencedirect.com/science/article/pii/S0306261916318098